Ab-intio based electron-phonon scattering for 2D materials within the NEGF framework

Gautam Gaddemane[1,2], Rutger Duflou[1,2], Kiroubanand Sankaran[1], Geoffrey Pourtois[1], Michel Houssa[1,2], and Aryan Afzalian[1]

[1]*imec, Kapeldreef 75, 3001 Leuven, Belgium*

[2] *KU Leuven, Laboratory of Semiconductor Physics, Celestijnenlaan 200 D, 3001 Leuven, Belgium*

gautam.gaddemane@imec.be

I. Introduction

For the last 15 years, two-dimensional (2D) materials are being actively studied as a possible replacement for silicon. Due to their layered nature, the materials can be scaled down to a single atomic layer, favouring extreme device scaling. In addition, surface effects such as roughness, dangling bonds, and interface states are also reduced/eliminated [1], [2]. Besides, these materials confine charge carriers to atomic-thin layers, which provides excellent gate-control and reduces short-channel effects [3]. Graphene (single layer graphite) was the first of the 2D material to be isolated, and very high electron mobility ($>10^5$ cm^2/Vs) in its suspended state was reported [4]. However, it does not have a bandgap, which is a severe limitation for transistor applications (challenging to turn off the device). Still, it initiated the discovery of other 2D materials with a band gap, such as phosphorene (mono- or few-layer black phosphorous) [5] and transition metal dichalcogenides (TMDs) [6]. However, TMDs and phosphorene are found to have lower intrinsic mobility when compared to graphene [7], [8]. This can be attributed to the large electron-phonon scattering present in these materials. Theoretical calculations have predicted that, even in 2D material-based transistors of channel lengths as small as about 5 nm, electron-phonon scattering plays a significant role [9], [10].

To study the performance of 2D material-based devices, quantum transport models, such as the non-equilibrium Green's function (NEGF) approach, are being developed to consider both the non-equilibrium and quantum effects. Currently, the calculations performed for 2D materials include scattering processes by approximating the self-energy terms with constant deformation potentials calculated using the Bardeen-Shockley approach (energy shift of the band edge under isotropic strain) [11], which has shown to overestimate the carrier mobility [8]. Another approach was adopted by Lee et al. [12], where they scaled the self-energy terms in the NEGF framework to fit the electron mobility obtained from semiclassical models.

Our current work proposes an analytical approach of extracting scattering parameters directly from full electron-phonon matrix elements (calculated from first-principles) rather than strained band structure calculations. These parameters are then implemented in the NEGF formalism through the self-energy terms. Considering monolayer tungsten disulfide (ML-WS_2) as an example, we verify these parameters' validity by comparing the electron mobility obtained from the NEGF method to the one obtained from the semiclassical linearized-Boltzmann transport equation (LBTE).

II. Methods and Results

We use our in-house developed Real-Space NEGF solver, ATOMOS [9], [13] for our transport calculations. It is a dissipative NEGF solver based on the recursive Green's function (RGF) algorithm [14].

The electronic states are calculated from density functional theory (DFT) as implemented in the Quantum Espresso package [15]. The Bloch states obtained are then transformed into maximally-localized Wannier functions (MLWF), which are centred on the ions, using Wannier90 code [16]. For the DFT calculations, we use Perdew-Burke-Enzerhoff generalized gradient approximation (GGA-PBE) for the exchange-correlation functional [17] and Ultrasoft pseudopotentials. The resulting information, including atomic positions, lattice vectors and localized tight-binding type Hamiltonian matrix elements are used to build full-device structure.

Electron-phonon scattering is included in the NEGF formalism through the self-consistent Born approximation [18]. Assuming that the phonons stay in equilibrium, the scattering self-energy term ($\Sigma^<(E)$) is written as [9]:

$$\Sigma^<(E) = \sum_{\mathbf{q}} |M_{\mathbf{q}}|^2 [(N_{\mathbf{q}}+1)G^<(E+\hbar\omega_{\mathbf{q}}) + N_{\mathbf{q}} G^<(E-\hbar\omega_{\mathbf{q}})], \tag{1}$$

where $M_{\mathbf{q}}$ is the electron-phonon coupling matrix element in the localized-orbital basis, $G^<$ is the lesser Green's function, $N_{\mathbf{q}}$ is the Bose-Einstein distribution, E is the scalar electron energy and $\omega_{\mathbf{q}}$ is the phonon frequency.

Our approach includes elastic and inelastic scattering by acoustic phonons and inelastic scattering by optical phonons by approximating the self-energy terms with analytical expressions [9]. For elastic acoustic phonon scattering, the self-energy term can be approximated as:

$$\Sigma^<_{\text{elastic}} = M^2_{\text{elastic}} G^<(E), \tag{2}$$

978-1-6654-0685-7/21/$31.00 ©2021 IEEE

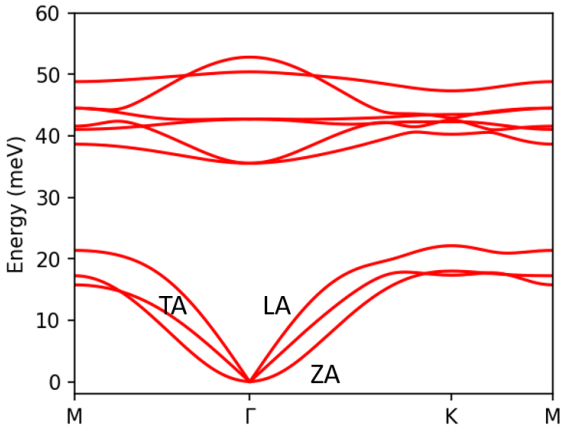

Fig. 1. Phonon dispersion of ML-WS_2 plotted along the high-symmetry lines.

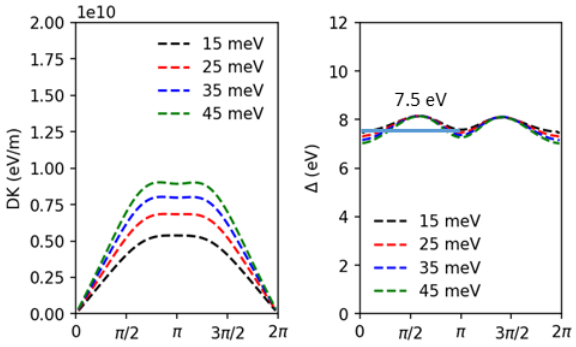

Fig. 2. DK and Δ_{elastic} plotted for LA phonons as a function of the angle of the final wavevector formed with respect to $\Gamma - K$ direction.

with

$$M^2_{\text{elastic}} = \frac{\Delta^2_{\text{elastic}} k_B T}{\rho V v^2_{\text{p}}}, \tag{3}$$

where Δ_{elastic} (eV) is called the "effective" deformation potential for elastic acoustic phonon scattering, ρ is the mass density, V is the mesh volume, v_{p} is the sound velocity. The above expression is valid only for acoustic modes with a linear dispersion near the Γ symmetry point. As shown later, for 2D materials, only the in-plane acoustic phonons (TA and LA) have a linear dispersion. The out-of-plane acoustic phonons or ZA phonons have a parabolic dispersion and in certain 2D materials (silicene, germanene), which lack horizontal (σ_{h}) mirror symmetry, electron-ZA phonon scattering is significant [19]. However, in most of the 2D materials of interest, such as 2H-TMDs and phosphorene coupling to ZA phonons is found to be negligible thanks to the σ_{h} mirror symmetry [20].

The self-energy term for inelastic scattering by acoustic and optical phonons can be approximated as:

$$\Sigma^{<}_{\text{inelastic}} = M^2_{\text{inelastic}} \left(N_B + \frac{1}{2} \pm \frac{1}{2} \right) G^{<}(E \pm E_{\text{ph}}), \tag{4}$$

with

$$M^2_{\text{inelastic}} = \frac{\Delta^2_{\text{inelastic}} \hbar^2}{2\rho V E_{\text{ph}}}, \tag{5}$$

where $\Delta_{\text{inelastic}}$ (eV/m) is the "effective" deformation potential for inelastic scattering, E_{ph} is the optical phonon energy or the zone edge acoustic phonon energy, and N_B is the Bose-Einstein distribution calculated at constant phonon energy E_{ph}. The parameters (Δ_{elastic}, $\Delta_{\text{inelastic}}$, E_{ph} and v_{p}) needed to evaluate M_{elastic} and $M_{\text{inelastic}}$ can be extracted from the full phonon dispersion and electron-phonon matrix elements, which can be calculated using the density functional perturbation theory (DFPT) approach [15], [21]. Considering ML-WS_2 as an example, we show below the procedure to extract these parameters.

In Fig 1, we show the phonon dispersion calculated for ML-WS_2 using the DFPT approach as implemented by the Quantum Espresso software package [15], [22]. ML-WS_2 has nine phonon branches, three acoustic and six optical branches. As mentioned above, the ZA phonons has a parabolic dispersion near the Γ symmetry point. The coupling between electrons and ZA phonons is negligible in ML-WS_2 due to σ_{h} mirror symmetry. Parameters such as E_{ph} and v_{p} are extracted from the phonon dispersion.

The plane-wave based electron-phonon coupling matrix elements calculated from DFPT are of the form:

$$M_{mn\lambda}(\mathbf{k}, \mathbf{q}) = \left(\frac{\hbar}{2M_{cell}\omega_{\mathbf{q}\lambda}} \right)^{1/2} DK_{mn\lambda}(\mathbf{k}, \mathbf{q}), \tag{6}$$

where $\mathbf{k}$ and $\mathbf{k}' = \mathbf{k} - \mathbf{q}$ are the intial and final electron wavevector, $\mathbf{q}$ is the corresponding phonon vector, λ denotes different phonon modes, m and n are the initial and final band indices, M_{cell} is the total mass of the unit cell and DK is called the deformation potential. For small $\mathbf{q}$ vectors (elastic scattering regime), DK and Δ_{elastic} for in-plane acoustic phonons can be related as: $DK \approx \Delta_{\text{elastic}}|\mathbf{q}|$. Therefore, to extract Δ_{elastic}, we calculate DK from the matrix elements, for the same initial and final electron energies (taking initial wavevector $\mathbf{k}$ and final wavevector $\mathbf{k}'$ on an equienergy surface), as functions of the scattering angle (angle of the final wavevector $\mathbf{k}'$ formed with respect to the direction of the initial wavevector $\mathbf{k}$.). Δ_{elastic} is then obtained by dividing DK by the magnitude of the phonon wavevector ($|\mathbf{q}|$). In Fig 2 we show DK and Δ_{elastic} plotted as a function of the scattering angle for monolayer WS_2. We find that Δ_{elastic} can be approximated as a constant due to isotropic band structure in WS_2.

For inelastic phonon scattering, $DK \approx \Delta_{\text{inelastic}}$. Therefore, we calculate DK from the matrix elements for optical phonons and zone edge acoustic phonons by considering an initial wavevector $\mathbf{k}$ at the conduction band minima and the final wavevector $\mathbf{k}'$ on an equienergy surface of energy equal to the constant phonon energy E_{ph}. In Fig. 3, we show $\Delta_{\text{inelastic}}$ for two major contributing optical phonons and their corresponding phonon energies, E_{ph} in WS_2. Similarly, in

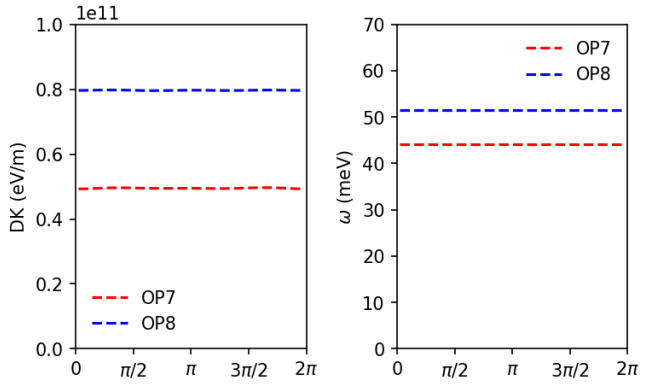

Fig. 3. DK and $\omega_{\mathbf{q}}$ for optical phonons plotted as a function of the angle of the final wavevector formed with respect to $\Gamma - K$ direction.

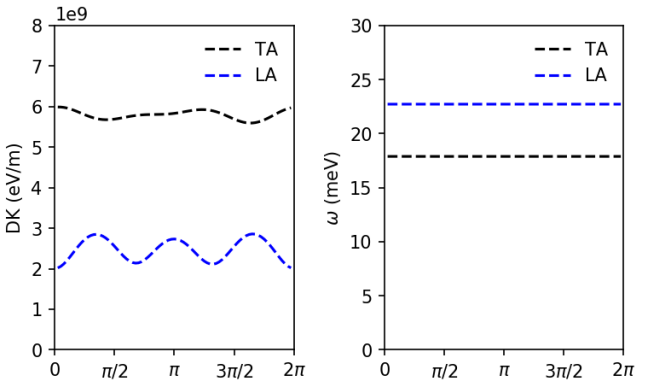

Fig. 4. DK and $\omega_{\mathbf{q}}$ for zone-edge acoustic phonons plotted as a function of the angle of the final wavevector formed with respect to $\Gamma - K$ direction.

Fig. II, we show $\Delta_{\text{inelastic}}$ for zone-edge acoustic phonons. In both cases, the DK obtained can be approximated as a constant over the scattering angle.

In Fig. 5, we show the mobility calculated from the NEGF approach by the dR/dL method [23] and intrinsic mobility calculated from LBTE using PERTURBO software [21]. The LBTE method uses full-bands and full electron-phonon scattering matrix elements(from first-principles calculations) to calculate electron mobility. The results are found to be in good agreement between both methods.

Our analytical approach is computationally efficient and can be a good approximation for constant "effective" deformation potentials. The deformation potentials can be approximated as constants for 2D materials with isotropic band structures, such as 2H-TMDs. However, in the case of anisotropic 2D materials like phosphorene, the deformation potentials have an angular dependence. In addition, for 2D materials which lack σ_{h} symmetry, the coupling with ZA phonons is not negligible. Therefore, we are currently working on implementing full electron-phonon matrix elements in the NEGF framework to study these materials accurately.

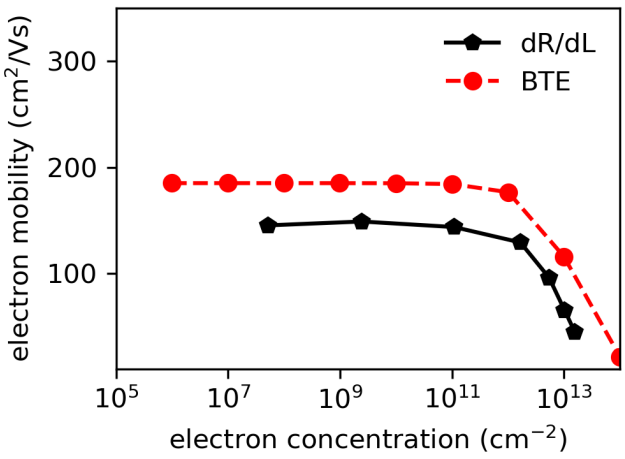

Fig. 5. Electron mobility for ML-WS_2 calculated from dR/dL method and LBTE.

References

[1] F. Schwierz, J. Pezoldt, and R. Granzner, "Two-dimensional materials and their prospects in transistor electronics," *Nanoscale*, vol. 7, no. 18, pp. 8261–8283, 2015.

[2] M. Chhowalla, D. Jena, and H. Zhang, "Two-dimensional semiconductors for transistors," *Nature Reviews Materials*, vol. 1, no. 11, pp. 1–15, 2016.

[3] J. Xu, L. Chen, Y.-W. Dai, Q. Cao, Q.-Q. Sun, S.-J. Ding, H. Zhu, and D. W. Zhang, "A two-dimensional semiconductor transistor with boosted gate control and sensing ability," *Science advances*, vol. 3, no. 5, p. e1602246, 2017.

[4] K. I. Bolotin, K. J. Sikes, Z. Jiang, M. Klima, G. Fudenberg, J. e. Hone, P. Kim, and H. Stormer, "Ultrahigh electron mobility in suspended graphene," *Solid state communications*, vol. 146, no. 9-10, pp. 351–355, 2008.

[5] L. Kou, C. Chen, and S. C. Smith, "Phosphorene: fabrication, properties, and applications," *The journal of physical chemistry letters*, vol. 6, no. 14, pp. 2794–2805, 2015.

[6] S. Manzeli, D. Ovchinnikov, D. Pasquier, O. V. Yazyev, and A. Kis, "2d transition metal dichalcogenides," *Nature Reviews Materials*, vol. 2, no. 8, p. 17033, 2017.

[7] Z. Jin, X. Li, J. T. Mullen, and K. W. Kim, "Intrinsic transport properties of electrons and holes in monolayer transition-metal dichalcogenides," *Physical Review B*, vol. 90, no. 4, p. 045422, 2014.

[8] G. Gaddemane, W. G. Vandenberghe, M. L. Van de Put, S. Chen, S. Tiwari, E. Chen, and M. V. Fischetti, "Theoretical studies of electronic transport in monolayer and bilayer phosphorene: A critical overview," *Physical Review B*, vol. 98, no. 11, p. 115416, 2018.

[9] A. Afzalian, "Ab initio perspective of ultra-scaled cmos from 2d-material fundamentals to dynamically doped transistors," *npj 2D Materials and Applications*, vol. 5, no. 1, pp. 1–13, 2021.

[10] G. Gaddemane, M. L. Van de Put, W. G. Vandenberghe, E. Chen, and M. V. Fischetti, "Monte carlo analysis of phosphorene nanotransistors," *Journal of Computational Electronics*, vol. 20, no. 1, pp. 60–69, 2021.

[11] A. Szabo, R. Rhyner, and M. Luisier, "Ab-initio simulations of mos 2 transistors: From mobility calculation to device performance evaluation," in *2014 IEEE International Electron Devices Meeting*. IEEE, 2014, pp. 30–4.

[12] Y. Lee, S. Fiore, and M. Luisier, "Ab initio mobility of single-layer mos 2 and ws 2: comparison to experiments and impact on the device characteristics," in *2019 IEEE International Electron Devices Meeting (IEDM)*. IEEE, 2019, pp. 24–4.

[13] A. Afzalian, E. Akhoundi, G. Gaddemane, R. Duflou, and M. Houssa, "Advanced dft-negf transport techniques for novel 2-d material and device exploration including hfs2/wse2 van der waals heterojunction tfet and wte2/ws2 metal/semiconductor contact," *IEEE Transactions on Electron Devices*, 2021, doi: 10.1109/TED.2021.3078412.

[14] A. Svizhenko, M. Anantram, T. Govindan, B. Biegel, and R. Venugopal, "Two-dimensional quantum mechanical modeling of nanotransistors," *Journal of Applied Physics*, vol. 91, no. 4, pp. 2343–2354, 2002.

[15] P. Giannozzi, S. Baroni, N. Bonini, M. Calandra, R. Car, C. Cavazzoni, D. Ceresoli, G. L. Chiarotti, M. Cococcioni, I. Dabo *et al.*, "Quantum espresso: a modular and open-source software project for quantum simulations of materials," *Journal of physics: Condensed matter*, vol. 21, no. 39, p. 395502, 2009.

[16] A. A. Mostofi, J. R. Yates, Y.-S. Lee, I. Souza, D. Vanderbilt, and N. Marzari, "wannier90: A tool for obtaining maximally-localised wannier functions," *Computer physics communications*, vol. 178, no. 9, pp. 685–699, 2008.

[17] J. Klimeš, D. R. Bowler, and A. Michaelides, "Chemical accuracy for the van der waals density functional," *Journal of Physics: Condensed Matter*, vol. 22, no. 2, p. 022201, 2009.

[18] A. Afzalian, "Computationally efficient self-consistent born approximation treatments of phonon scattering for coupled-mode space non-equilibrium green's function," *Journal of Applied Physics*, vol. 110, no. 9, p. 094517, 2011.

[19] G. Gaddemane, W. G. Vandenberghe, M. L. Van de Put, E. Chen, and M. V. Fischetti, "Monte-carlo study of electronic transport in non-σ h-symmetric two-dimensional materials: Silicene and germanene," *Journal of Applied Physics*, vol. 124, no. 4, p. 044306, 2018.

[20] M. V. Fischetti and W. G. Vandenberghe, "Mermin-wagner theorem, flexural modes, and degraded carrier mobility in two-dimensional crystals with broken horizontal mirror symmetry," *Physical Review B*, vol. 93, no. 15, p. 155413, 2016.

[21] J.-J. Zhou, J. Park, I.-T. Lu, I. Maliyov, X. Tong, and M. Bernardi, "Perturbo: A software package for ab initio electron–phonon interactions, charge transport and ultrafast dynamics," *Computer Physics Communications*, p. 107970, 2021.

[22] P. Giannozzi, O. Andreussi, T. Brumme, O. Bunau, M. B. Nardelli, M. Calandra, R. Car, C. Cavazzoni, D. Ceresoli, M. Cococcioni *et al.*, "Advanced capabilities for materials modelling with quantum espresso," *Journal of physics: Condensed matter*, vol. 29, no. 46, p. 465901, 2017.

[23] K. Rim, S. Narasimha, M. Longstreet, A. Mocuta, and J. Cai, "Low field mobility characteristics of sub-100 nm unstrained and strained si mosfets," in *Digest. International Electron Devices Meeting,*. IEEE, 2002, pp. 43–46.